Hybrid, multi-megawatt, medium frequency HVDC transformer for offshore wind turbines

Hybrid, multi-megawatt, medium frequency HVDC transformer for offshore wind turbines

M. Smailes, C. Ng, J. Shek, M. Abusara, G. Theotokatos, P. Mckeever

IDCORE, UK M.Smailes@ed.ac.uk, Narec, UK Chong.Ng@Narec.co.uk, The University of Edinburgh, UK J.Shek@ed.ac.uk, The University of Exeter, UK M.Abusara@exeter.ac.uk, The University of Strathclyde, UK Gerasimos.Theotokatos@strath.ac.uk, Narec, UK Paul.Mckeever@Narec.co.uk

Keywords: 5 words max

Abstract

As the offshore wind industry moves further offshore HVDC transmission is becoming increasingly popular. HVDC transformer substations are not optimised for offshore industry however, increasing costs and reducing redundancy. A modular HVDC transformer located within each wind turbine nacelle could mitigate these problems however, careful design is required to minimise losses. For example the converter topology will influence the semi-conductor and magnetic transformer losses. In this paper several transformer configurations comprising combinations of the H-Bridge and Modular Multilevel Converter topologies are modelled in the Matlab/Simulink environment. The configurations are evaluated for use in a medium frequency HVDC transformer based on their contribution to total losses, their stability and range of real and reactive power control.

1 Introduction

The trend for offshore wind farms to move further offshore, combined with the falling cost of power electronics has resulted in an increase in the number of wind farms using HVDC systems for power transmission to shore [1], [2]. The HVDC converters in use today however, are not optimised for the offshore wind industry, offering little in terms of system redundancy and accounting for roughly 11% of their capital costs [3], [4]. A modular, high power, Medium Frequency (MF = 500 – 2000 Hz), hybrid HVDC transformer (Fig 1) has therefore been proposed in [5] to address these issues. The voltage is stepped up and converted to HVDC for parallel grid connection within the turbine nacelle, negating the requirement for an offshore platform. Redundancy is also increased due to the modular design and inter-array cable losses are minimised. By operating in the MF range the transformer's size and weight are minimised, simplifying the turbine's installation and foundation design.

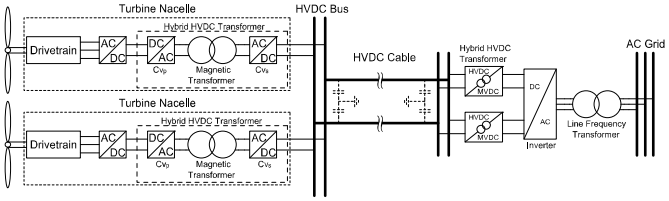

Fig 1: Offshore wind farm using proposed hybrid HVDC transformer design

Medium Frequency Power Transformers (MFPT) for high voltages and turns ratios have been shown to be difficult to design however [6]. The inter-winding and lamination capacitance can no longer be ignored and harmonics on the input waveform cause increased core losses [7], [8]. Winding losses are compounded by the high turns ratio required to connect directly to a parallel HVDC grid. The voltage and flux waveforms may therefore play a more significant role in the magnetic losses. The work conducted previously in this area has focused on optimising the magnetic transformer design [9], [10] or switching algorithms [11] but not the converter topology. As the converter topology contributes to the shape of the voltage waveforms, it too may have a significant effect on the overall losses of the transformer. Several converter topologies exist in the literature including the Neutral Point Clamp (NPC) and Cascade H-Bridge (CHB) however, they are unsuitable for the hybrid HVDC converter. The NPC is known to be unstable [12], requiring complex additional circuitry to balance capacitor voltages. Moreover, multiple voltage sources are required for the CHB, which are not available within a HVDC network. Both the H-Bridge (HB) and Modular Multilevel Converter (MMC) however, are well suited for this application. The HB has a simple and robust design while the MMC can generate a near perfect sine wave potentially lowering the magnetic transformer losses.

The aim of the paper is to investigate the effect of converter topology on the transformer losses and hence determine the optimum configuration for the hybrid HVDC transformer. To this end, the hybrid HVDC transformer was modelled in Matlab/Simulink using various configurations of the MMC and HB topologies. The models were run over the MF range and each configuration evaluated based on their contribution to total losses, their stability and range of real and reactive power control. Core and converter losses are considered in the analysis however, core optimisation and winding losses are not considered.

Section 2 describes the creation of the Simulink/Matlab models, the results of which are in Section 3. The results are discussed in Section 4 and conclusions drawn in Section 5.

2 Computer Model

The models are designed for a fictional 6.5 MW wind turbine with a nominal 6.5 kV LVDC bus voltage (V_{in}) between the fully rated generator rectifier and hybrid transformer. Steady state operation at rated power is assumed through out the simulations with the generator rectifier allowing variable

speed turbine operation. The transformer output connects to a fictional ±300 kV HVDC network via a shunt connection.

The configurations of the model can be split into three groups. In the first, HB converters are used for both primary (CS_p) and secondary (CS_s) and converters as shown in Fig 3 with MMCs used in the second, Fig 4 and are referred to as the full HB and full MMC respectively. In the third group a HB is used on the CS_p with a MMC used on the CS_s. The control algorithms for output power, P_{out} and transformer reactive power, Q_T regulation for all three groups is shown in Fig 2. The LVDC bus and HVDC cable resistances are represented by R_b and R_c respectively. The transformer has a 1:100 turns ratio with the total lumped transformer inductance located on the primary side of L_T = 0.1 mH and was selected using (1).

Fig 2: Real and reactive power control algorithms

$$P=\frac{V_1 V_2 \sin\delta}{X_T} \quad (1)$$

Here P is the power transferred, X_T is the lumped transformer reactance and δ is the load angle, V_1 and V_2 are V_p and V_s respectively referred to the primary side. (1) is used to chose L_T such that it is small enough to allow 6.5 MW to be transferred but large enough to maintain stability in control of P_{out}. In all models, each IGBT represents a valve as shown in Fig 3 containing a number of series S_{rows} and parallel P_{paths} IGBTs to resist the voltage and current stresses experienced by the valve.

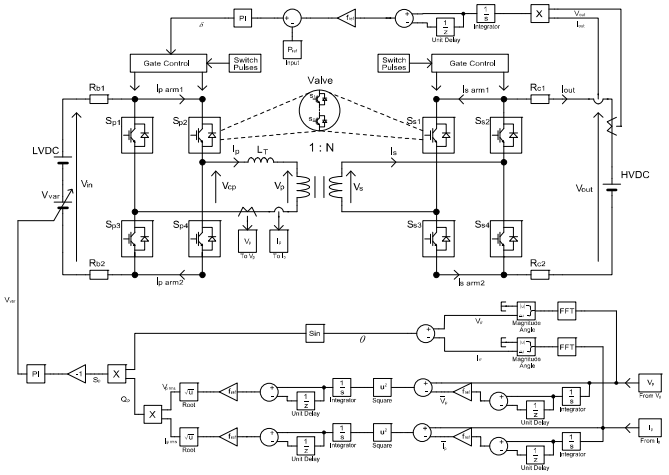

Fig 3: Detailed HB model and closed loop control

The HB is controlled to have 3 levels (3L) and a duty ratio of D = 0.33, so as to minimise the induced harmonics. The primary gate control circuit has an additional input to control the output power of the Hybrid HVDC Transformer. The output power (P_{out}) is calculated from:

$$P_{out}=f_{ref}\int V_{out} I_{out} \cdot dt \quad (2)$$

Which is then compared to a reference value and the difference used to control the delay angle of the primary converter and hence δ and power flow according to (1). To minimise the volume and losses of the transformer it is necessary to maintain a power factor, pf ≈ 1, necessitating the control of reactive power. However, calculating reactive power is complicated by unpredictable and highly non-sinusoidal nature of V_p and I_p. The phase angle (θ) cannot be determined directly in the time domain and their magnitudes are often inaccurate when calculated in the frequency domain. θ was therefore calculated in the frequency domain through use of a Fast Fourier Transform (FFT) and the apparent power S_T calculated in the time domain (3).

$$S_T=\sqrt{f_{ref}\int\left[\left(V_p-f_{ref}\int V_p\cdot dt\right)^2\cdot\left(I_p-f_{ref}\int I_p\cdot dt\right)^2\cdot dt\right]} \quad (3)$$

The mean of V_p and I_p is subtracted from the waveforms to eliminate any DC component present. The reactive power in the transformer, Q_T can then be found in the usual manner. This is compared to zero and used to regulate the LVDC bus voltage and compensate for Q_T, Fig 3 and Fig 4. In practice this can be achieved by changing the power flow through the transformer in relation to the power generated by the wind turbine, decreasing power flow increases LVDC bus voltage and vice versa. In the models using a variable DC source simulates this. Alternatively the duty ratio of the primary and secondary converters could be control the reactive power flow. This however, may increase the harmonic content of the transformer and so is not preferred.

The same PQ control algorithms are used in the MMC model however, the switching pulse input to the gate control differs. It is well known that the capacitor voltages (V_c) within the MMC modules can vary if not balanced properly. Multiple switch combinations are possible for voltage outputs other than the maximum or minimum and Snx is always the inverse of Sn, as demonstrated for a 3L MMC in Table 1. The module is said to be switched in or on if Snx is conducting, while if Sn is conducting the module is bypassed or off. The module capacitor voltages can therefore be controlled as follows: If a module is switched in and the arm current (I_{arm}) is positive the capacitor voltage will rise while if it is negative the capacitor will discharge as shown in the flow diagram (Fig 5).

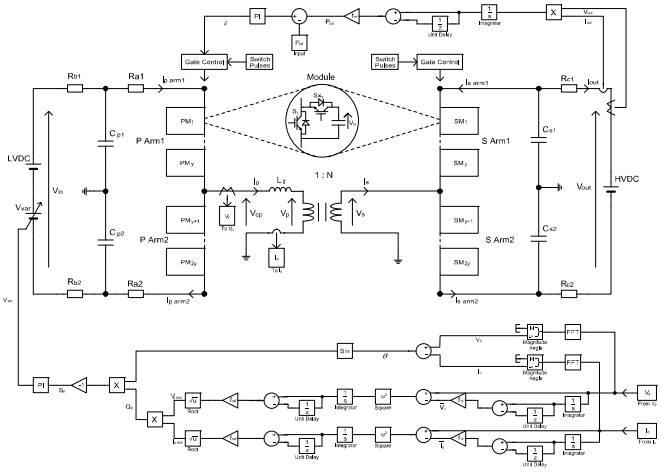

Fig 4: Detailed MMC model and closed loop control

The results from the model simulations were exported to Matlab where the average steady state conduction, switching and core losses were calculated. Several IGBT switch options were evaluated and fast switching IGBT modules were found to have the lowest overall converter losses due the greatly reduced switching losses in the MF range. The Infineon FD300R12KS4_B5 switch with collector emitter rated voltage V_{ce} = 1.2 kV and collector rated current I_c = 400A was selected as it provides a good balance between low loss and practicality. The same switches are used in both CS_p and CS_s to reduce the parts inventory and hence capital and maintenance costs. The IGBT junction temperatures are assumed to be constant at 125 °C throughout the steady state operation. In reality the operating temperature may vary but it would be close to the maximum operating temperature.

Valve	Logic				
S1	1	1	1	0	1
	0	1	0	0	0
S2	0	1	0	0	0
	1	1	1	0	1
S3	1	0	1	1	1
	0	0	0	1	0
S4	0	0	0	1	0
	1	0	1	1	1
S1x	0	1	0	0	0
	1	1	1	0	1
S2x	1	1	1	0	1
	0	1	0	0	0
S3x	0	0	0	1	0
	1	0	1	1	1
S4x	1	0	1	1	1
	0	0	0	1	0
1					
0					
-1					

Table 1: Switching pattern for a 3L MMC

The on resistance R_{on} and switching loss of semiconductors is not constant but rather varies with I_c and the relationship provided by the switch manufacturer. Simulink does not offer enough parameters to account for this accurately and so ideal switches were used in the simulations and the voltage drop and switching loss in each valve determined separately from the corresponding I_c and the datasheet.

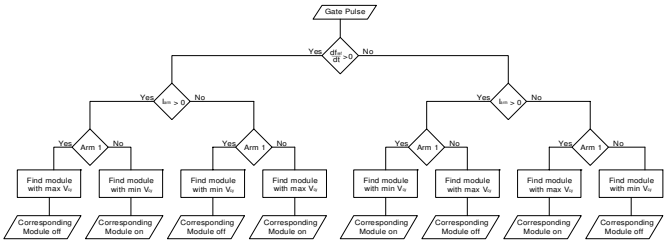

Fig 5: Flow diagram of module capacitor voltage balancing algorithm for MMC

The conduction power loss (P_{con}) is then calculated from:

$$ES_{con} = \sum I_{c\,i,n} \cdot VS_{i,n} \cdot T_{step} \tag{4}$$

$$ED_{con} = \sum Ic_{i,n} \cdot VD_{i,n} \cdot T_{step} \tag{5}$$

$$P_{con} = P_{paths} S_{rows} \cdot \frac{(ES_{con} + ED_{con})}{T_{cycle}} \tag{6}$$

Where; ES_{con} and ED_{con} are the IGBT and diode conduction energy losses, T_{step} is the period between each time step and T_{cycle} is the period over which the energy calculation took place and $VS_{i,n}$ is the voltage dropped across the n^{th} switch at over the i^{th} T_{step}.

A switching operation occurs when either an IGBT or diode turns on ie. when I_c increases or decreases from 0 A respectively and the total switching loss(P_{switch}) can then be calculated from :

$$ESs_{total} = \sum E_{IGBT\,i,n} \tag{7}$$

$$EDs_{total} = \sum E_{diode_i,n} \tag{8}$$

$$P_{switch} = \frac{EDs_{total} + ESs_{total}}{t_{cycle}} \tag{9}$$

Where ESs_{total} is the energy lost in all the IGBTs, EDs_{total} is the total reverse recovery energy from all the diodes and E_{IGBT} and E_{Diode} represent the energy lost in each switching operation for the corresponding I_c.

The chosen magnetic transformer core for the simulation is the Magnetics' Material F as it has been designed to operate in the MF range. The core loss has been calculated using the Steinmetz Equation (SE)

$$P_{core} = k f_{ref}^{\alpha} \hat{B}^{\beta} \tag{10}$$

Where P_{core} is the magnetic core loss per unit volume, $\hat{B}$ is the peak flux density and k, α and β, are material constants termed the Steinmetz Parameters. They are calculated as 180.4, 1.06 and 2.85 respectively by taking the logarithm of (10) to put it in a linear form and performing a 3D linear regression using the core loss data provided by the manufacturer. As (10) is only valid for sinusoidal waveforms, a Fourier analysis has been performed on the B waveform. The core loss can then be calculated for each frequency component and summed using vector addition to give the total core loss. It has been noted in the literature [13] that this approach is not mathematically accurate as the SE is non-linear. However it has been used here since $\hat{B}$ is constant, α is close to unity and only a rough estimate is required. B has been calculated using V_p and it is assumed that (11) is valid for non-sinusoidal waveforms and when the primary and secondary waveforms differ.

$$B = \frac{V_p}{A_e n_p f_{ref}} \tag{11}$$

In (11) A_e is the minimum core area permitted at each frequency and n_p is the number of turns on the primary.

3 Results

The simulation results of the three hybrid transformer configurations are presented here. Only one set of simulations are run for the full HB and HB-MMC groups however, the full MMC group contains multiple sets. Here 7L and 11L CS_ps are modelled with an 11L CS_s and a 25L CS_s is

modelled with an 11L CS_p. The configurations can then be evaluated for use in the hybrid HVDC transformer based on the converter and core efficiency and the range and stability of P_{out} and Q_T.

3.1 Real Power Control

In Fig 6 the sensitivity of P_{out} with respect to δ may be seen for each configuration at 500 Hz. The gradient of the full HB and HB MMC combination is much greater than that of the full MMC configurations. As a result small changes in δ correspond to great variations in P_{out} creating an unstable device. In the full MMC configuration the lower gradient corresponds to a greater stability in P_{out}. Moreover, as the number of voltage levels increases, stability improves further. It can be seen however, that increasing the number of levels in the CS_s has a much smaller impact on the stability of P_{out}. It can be seen however, that as the difference between the voltage levels on the CS_p and CS_s increases some of the lower level range in P_{out} is lost.

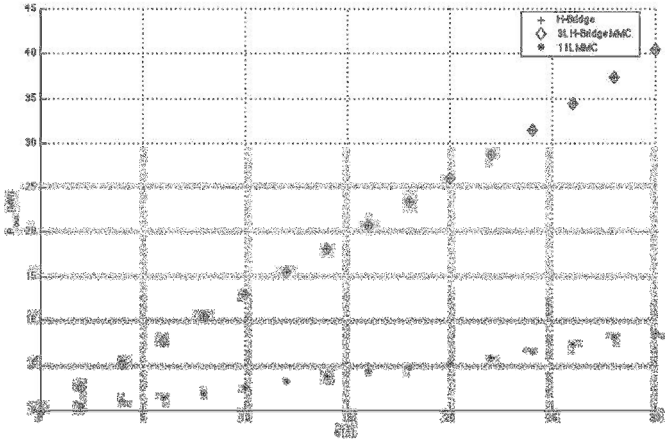

Fig 6: Power output for MMC and HB configurations vs. increasing load angles.

3.2 Reactive Power Control

Reactive power control is achieved in the model simulations by increasing the LVDC bus voltage. Therefore the level of Q_T compensation required can be seen by the change in the LVDC bus voltage from its nominal value. The normalised increase in LVDC bus voltage is therefore plotted against increasing frequencies for each transformer configuration in Fig 7. It can be seen that as frequency increases the level of Q_T compensation increases for all configurations however, the full HB and HB-MMC combination require significantly less. At their maximum the full HB and HB-MMC LVDC bus voltage increases by about 10% compared to around 110% for the full MMC case. Moreover, increasing either the voltage levels on the CS_p or CS_s has no effect on the level of compensation required.

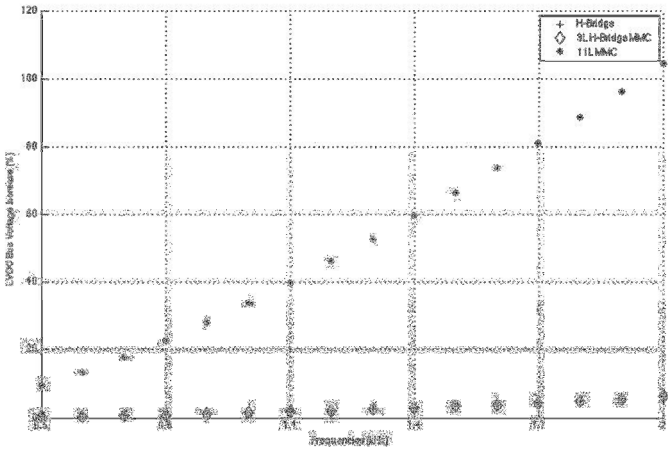

Fig 7: Voltage increase required for Q_T compensation vs. increasing frequencies.

3.3 Losses

The normalised converter and magnetic core losses for each transformer configuration have been calculated across the MF range and are shown in Fig 8 and Fig 9 respectively. The full HB has the lowest converter losses, closely followed by the HB-MMC combination. At 500 Hz the 7L CS_p 11L CS_s MMC losses are very close to those of the full H-Bridge however, they increase significantly at 600 Hz. Similarly the difference in losses between the 11L CS_p 11L CS_s decrease up to 1700 Hz but then sharply increase. These arise as the MMC topologies approach and then exceed the optimum number of primary voltage levels for a given LVDC bus voltage. This optimum number of voltage levels (OVL) is defined as the minimum number of voltage levels required such that the voltage stress across each valve does not exceed that of the rated value of one IBGT. It may also be seen that increasing the number of voltage levels on the CS_s as a negligible impact on converter losses as it is operating well below the CL.

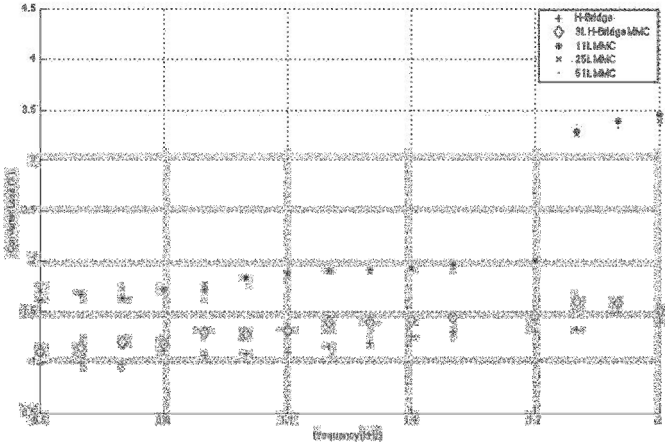

Fig 8: Calculated converter losses for configurations 1 – 4 over the MF range

While the converter losses for the full HB and HB-MMC are lower than those of the full MMC the core losses are smaller for the MMC topologies and decrease as the number of

voltage levels increase in the CS_p. Once again however, increasing the number of voltage levels on the CS_p has no effect of the calculated losses.

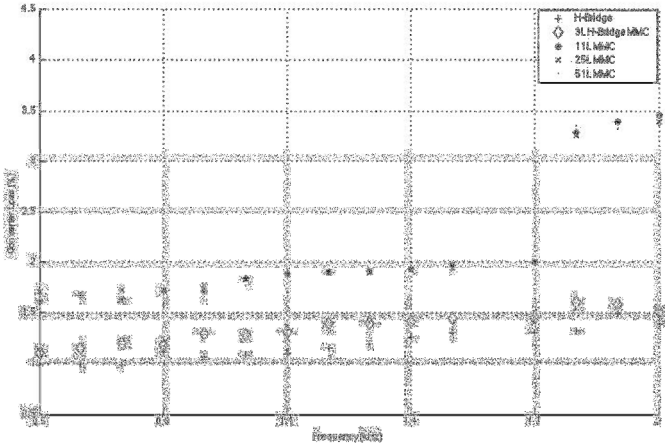

Fig 9: Normalised transformer core losses per unit volume for each configuration vs. frequency

4 Discussion

In (Fig 10) the voltage and current waveforms at the primary side of the magnetic transformer can be seen. It is clear that a small increase in δ will correspond to a large increase in I_p and hence P_{out}. However, with the higher number of voltage levels in the MMC configurations, increasing δ corresponds to a smaller voltage drop across L_T and hence a smaller increase in P_{out}. As the difference in the number of voltage levels between the primary and secondary increases, the lower range of P_{out} decreases. This is likely due to the difference in harmonic make-up between the CS_p and CS_s resulting in an increase in reactive power flow and a loss of control in P_{out}. The range and stability of P_{out} through the transformer is vital to maximise efficiency and revenues of the wind turbine and so the full MMC configuration does have some significant advantages over the others.

It is estimated however, that the maximum deviation from the LVDC bus voltage should be no more than ±15 %. This would limit the operational frequency of the MMC to around 700 Hz, as above this, the required Q_T compensation would exceed the capabilities of the transformer. If this limit is exceeded reactive power will begin to flow in the magnetic transformer increasing its volume and losses.

While the full HB has the lowest converter losses its core losses are the greatest along side the HB-MMC combination. If it is assumed however, that the core volume is $1m^3$ at 500 Hz (roughly twice that of [9]) then the total transformer loss at 500 Hz is 1.21% for the full HB and 1.32% for the full MMC and. Clearly then the converter losses are more significant than those of the transformer showing the importance of the converter design. In the literature [14] it is suggested that the MMC would have the lower losses however, these results were based on the HB using Pulse Width Modulation (PWM) to reduce the generated harmonics. Without using (PWM) the full HB has fewer losses but the MMC with the OVL on the CS_p is still recommended for 500-600 Hz due to the increased control.

While the HB-MMC offers no reduction in core loss, the turns ratio of the magnetic transformer may be halved as $\widehat{V_p} = LVDC$ while $\widehat{V_s} = 0.5 \cdot HVDC$. This may reduce the volume and losses associated with magnetic transformer as well as reducing its complexity. Additionally this provides the possibility to increase the number of voltage levels on the secondary with no increase in losses. While this was shown to have no effect on core loss it may prove to influence the winding losses. This however, is outwith of the scope of this paper and is an area for further study.

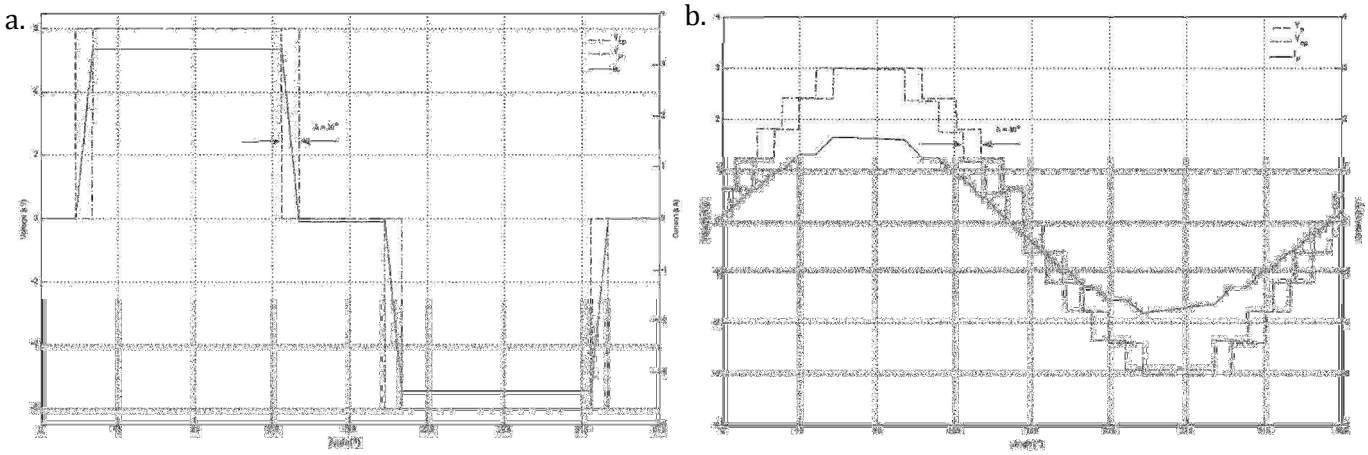

Fig 10: V_{cp}, V_p and resulting I_p waveforms for the HB (a) and 11L MMC (b) configurations

5 Conclusion

The hybrid HVDC transformer has been modelled in the Matlab/Simulink environment using full HB, full MMC and HB-MMC configurations The conduction and switching losses were calculated over the MF range and the stability and range of P_{out} and Q_T control evaluated for each configuration. Using a HB for both primary and secondary converters was found to have the lowest converter losses but have highly sensitive and limited P range control at low frequencies. A full MMC configuration restored P_{out} stability particularly with higher voltage levels on the CS_p however, deviating from the OVL on the primary significantly increased losses. Q_T control is limited at frequencies above 700 Hz limiting the full MMC to frequencies below this. The converter losses were found to influence the transformer losses more than the core losses and so the full HB is the preferred topology for operating frequencies above 700 Hz. Below this the increased P_{out} control of the full MMC compensates for the marginally higher losses.

The HB-MMC losses were found to be marginally higher than those for the HB however, the number of turns required in the magnetic transformer is halved. This may appreciably decrease the volume of the transformer and reduce losses. Moreover, additional voltage levels on the secondary would be possible, potentially further lowering the winding losses. To characterise the effect of increasing the secondary voltage levels, the model must be expanded to calculated core volume and winding losses. Further work will focus on expanding the model and developing methods to mitigate potential harmonic mismatches between the primary and secondary converters.

References

[1] B. Van Eeckhout, D. Van Hertem, M. Reza, K. Srivastava, and R. Belmans, "Economic comparison of VSC HVDC and HVAC as transmission system for a 300 MW offshore wind farm," *Eur. Trans. Electr. Power*, p. n/a–n/a, Jun. 2009.

[2] A. Arapogianni, J. Moccia, J. Wilkes, J. Guillet, P. Wilczek, J. Scola, and S. Azau, "The European Offshore Wind Industry - Key Treds and Statistics 2012." European Wind Energy Association, Jan-2013.

[3] "Offshore Wind: Nordzee Ost." European Commission, Oct-2013.

[4] P. Giller, "Multi-Contracting for the first project financing in the German Offshore Wind Market: Projekt Offshore Wind Farm Meerwind Sud/Ost [288 MW Offshore Wind Farm]," 03-Jan-2012.

[5] C. Ng and P. McKeever, "Next generation HVDC network for offshore renewable energy industry," in *10th IET International Conference on AC and DC Power Transmission (ACDC 2012)*, Birmingham, 2012, pp. 1–7.

[6] D. Jovcic, "Bidirectional, High-Power DC Transformer," *IEEE Trans. Power Deliv.*, vol. 24, no. 4, pp. 2276–2283, Oct. 2009.

[7] N. Denniston, A. M. Massoud, S. Ahmed, and P. N. Enjeti, "Multiple-Module High-Gain High-Voltage DC-DC Transformers for Offshore Wind Energy Systems," *IEEE Trans. Ind. Electron.*, vol. 58, no. 5, pp. 1877–1886, May 2011.

[8] H. Li, X. Bai, and J. Wu, "Study on modeling of high frequency power pulse transformer," in *Automation Congress, 2008. WAC 2008. World*, 2008, pp. 1–5.

[9] S. Meier, T. Kjellqvist, S. Norrga, and H.-P. Nee, "Design considerations for medium-frequency power transformers in offshore wind farms," in *13th European Conference on Power Electronics and Applications, 2009. EPE '09*, 2009, pp. 1–12.

[10] G. Ortiz, J. Biela, and J. W. Kolar, "Optimized design of medium frequency transformers with high isolation requirements," in *IECON 2010 - 36th Annual Conference on IEEE Industrial Electronics Society*, 2010, pp. 631–638.

[11] G. Ortiz, J. Biela, D. Bortis, and J. W. Kolar, "1 Megawatt, 20 kHz, isolated, bidirectional 12kV to 1.2kV DC-DC converter for renewable energy applications," in *Power Electronics Conference (IPEC), 2010 International*, 2010, pp. 3212–3219.

[12] N. Flourentzou, V. G. Agelidis, and G. D. Demetriades, "VSC-Based HVDC Power Transmission Systems: An Overview," *IEEE Trans. Power Electron.*, vol. 24, no. 3, pp. 592–602, Mar. 2009.

[13] M. Albach, T. Durbaum, and A. Brockmeyer, "Calculating core losses in transformers for arbitrary magnetizing currents a comparison of different approaches," in *, 27th Annual IEEE Power Electronics Specialists Conference, 1996. PESC '96 Record*, 1996, vol. 2, pp. 1463–1468 vol.2.

[14] Q. Tu and Z. Xu, "Power losses evaluation for modular multilevel converter with junction temperature feedback," in *Power and Energy Society General Meeting, 2011 IEEE*, 2011, pp. 1–7.